

1 **Biogeochemical variations at the Porcupine Abyssal**
2 **Plain Sustained Observatory (PAP-SO) in the northeast**
3 **Atlantic Ocean, from weekly to inter-annual time scales**

4
5 S. E. Hartman^{1,*}, Z.-P. Jiang², D. Turk^{3,4}, R. S. Lampitt¹, H. Frigstad⁵,
6 C. Ostle^{6,7} and U.Schuster⁸

7
8 [1] {National Oceanography Centre, Southampton, UK}

9 [2] {Ocean Collage, Zhejiang University, China}

10 [3] {Dalhousie University, Canada}

11 [4] {Lamont-Doherty Earth Observatory, Columbia University, NY, USA}

12 [5] {Norwegian Environment Agency, Strømsveien 96, 0663 Oslo, Norway}

13 [6] {Sir Alister Hardy Foundation for Ocean Science (SAHFOS), Plymouth, UK}

14 [7] {School of Environmental Sciences, University of East Anglia (UEA), UK}

15 [8] {University of Exeter, UK}

16
17 Correspondence to: S.E.Hartman (suh@noc. ac.uk)

18
19 **Abstract**

20 We present high-resolution autonomous measurements of carbon dioxide partial pres-
21 sure $p(\text{CO}_2)$ taken *in situ* at the Porcupine Abyssal Plain sustained observatory (PAP- SO) in
22 the northeast Atlantic (49° N, 16.5° W; water depth of 4850 m) for the period 2010 to 2012.
23 Measurements of $p(\text{CO}_2)$ made at 30 m depth on a sensor frame are compared with other
24 autonomous biogeochemical measurements at that depth (including chlorophyll a-

1 fluorescence and nitrate concentration data) to analyse weekly to seasonal controls on $p(\text{CO}_2)$
2 flux in the inter-gyre region of the North Atlantic. Comparisons are also made with *in situ*
3 regional time-series data from a ship of opportunity and mixed layer depth (MLD)
4 measurements from profiling Argo floats. There is a persistent under saturation of CO_2 in
5 surface waters throughout the year which gives rise to a perennial CO_2 sink. Comparison with
6 an earlier dataset collected at the site (2003 to 2005) confirms seasonal and inter-annual
7 changes in surface seawater chemistry. There is year-to-year variability in the timing of deep
8 winter mixing and the intensity of the spring bloom.

9 The 2010–2012 period shows an overall increase in $p(\text{CO}_2)$ values when compared to
10 the 2003–2005 period. This is despite similar surface temperature, wind speed and MLD
11 measurements between the two periods of time. Future work should incorporate daily CO_2
12 flux measurements made using CO_2 sensors at 1 m depth and the *in situ* wind speed data now
13 available from the UK Met Office Buoy.

14

15 Keywords: carbon dioxide, nitrate, time-series, mooring buoys, ship of opportunity

16

17 Regional Index terms: North East Atlantic, Porcupine Abyssal Plain; geographic
18 bounding co-ordinates 48° N - 50° N, 16° W - 17° W

19

20 **1 Introduction**

21 A persistent feature of the subpolar North Atlantic is under-saturation of carbon
22 dioxide (CO_2) in surface waters throughout the year, which gives rise to a perennial CO_2 sink
23 (Körtzinger et al., 2008). This makes the north east Atlantic a region of great importance in
24 the global carbon cycle. However, there is evidence for inter-annual variation in the CO_2 sink
25 ($1\text{--}3 \text{ mol m}^{-2} \text{ a}^{-1}$) due to changes in wintertime mixing and stratification (Schuster and
26 Watson, 2007). Changes in the amount of CO_2 absorbed by the ocean may have implications
27 for the global carbon cycle now and as a carbon sink in the future. Studies of the physical and
28 biological processes regulating surface water $p(\text{CO}_2)$ (partial pressure of CO_2) are required to
29 estimate future trends in the ability of the ocean to act as a sink for increasing CO_2 in the

1 atmosphere. Frequent observations from fixed positions are critical to make these calculations
2 (McGillicuddy et al., 1998).

3 Accurate, high-resolution, long-term datasets are offered by time series studies such
4 as the Porcupine Abyssal Plain sustained Observatory (PAP-SO) in the northeast Atlantic at
5 49° N, 16.5° W (4850 m water depth) where a fixed-point mooring has been in place since
6 2002 (Hartman et al., 2012). The PAP-SO is in the North Atlantic Drift Region, a
7 biogeographical province defined by deep winter convective mixing (Longhurst, 2006;
8 Monterey and Levitus, 1997). The surface mixed layer depth changes from 25 m in the
9 summer to over 400 m in winter. A twofold decrease in winter nitrate concentration over a
10 three year period from 2003 has been attributed to a combination of shallower winter
11 convective mixing and changes in surface circulation (Hartman et al., 2010). The PAP-SO is
12 in an area with relatively high wind speeds, frequently greater than 10 m s⁻¹. High wind
13 speeds have a significant effect on CO₂ flux (Takahashi et al., 2002). The CO₂ flux at the
14 PAP-SO was calculated from $p(\text{CO}_2)$, between 2003 and 2005 as a net flux into the ocean of
15 over 3 mol m⁻² a⁻¹ (Körtzinger et al., 2008). This is a significant sink compared with
16 subtropical time series sites such as ESTOC (near the Canary Islands, 29.17° N, 15.5° W),
17 which is an overall annual CO₂ source region (0.05 mol m⁻² a⁻¹, Gonzalez-Davila et al.,
18 2003).

19 Recently, the decline in North Atlantic CO₂ uptake from 1994/1995 to 2002–2005 has
20 been linked to a variation in the North Atlantic Oscillation (Schuster and Watson, 2008;
21 Padin et al., 2011). The decreased uptake may be a consequence of declining rates of
22 wintertime mixing and ventilation between surface and subsurface waters due to increasing
23 stratification. Enhanced stratification forms a barrier to nutrient exchange, which may result
24 in a progressive decline in primary production (Field et al., 1998), as was seen in the North
25 Atlantic between 1999 and 2004 (Behrenfeld et al., 2006). The observed decrease in nitrate
26 concentration and productivity in this region (Behrenfeld et al., 2006), may in turn affect the
27 oceanic uptake of $p(\text{CO}_2)$.

28 In this paper, we present recent year round time-series data of temperature, salinity,
29 nitrate concentration, chlorophyll a-fluorescence and $p(\text{CO}_2)$ collected from 30 m depth from
30 2010 to 2012. The data are compared with an earlier published dataset (from 2003 to 2005)
31 and additional $p(\text{CO}_2)$ measurements made from a ship of opportunity. The *in situ* dataset is
32 considered in relation to convective mixing processes using mixed layer depth (MLD)

1 estimates calculated from profiling Argo floats. The weekly air-sea CO₂ flux at the PAP-SO
2 site was calculated from *in situ* $p(\text{CO}_2)$ measurements and ancillary satellite wind speed
3 datasets. The objective of this study is to examine the biogeochemical variations at the PAP-
4 SO in the northeast Atlantic over different periods from weekly, seasonal to annual.

6 **2 Materials and methods**

7 **2.1 Study site**

8 The position of the Porcupine Abyssal Plain sustained observatory (PAP-SO) at 49°
9 N, 16.5° W is shown in Fig. 1. Lampitt et al. (2001) has summarised the hydrography,
10 meteorology and upper mixed layer dynamics in the region.

12 **2.2 *In Situ* data**

13 The instrumentation of the PAP-SO observatory has been described in detail by
14 Hartman et al., 2012 (see Table 1 and Fig. 1 therein) and is briefly summarized here. Since
15 2002 instruments on a mooring at the PAP-SO (49° N, 16.5° W) have recorded a suite of
16 biogeochemical parameters in the mixed layer. Measurements of nitrate concentration,
17 chlorophyll a-fluorescence and $p(\text{CO}_2)$, have been made using biogeochemical sensors on a
18 frame at a nominal depth of 30 m, often within the deep chlorophyll maxima. Between 2002
19 and 2007 the sensor frame depth varied from 20 m to 225 m, deflecting in response to local
20 currents. A surface buoy was added in 2007 so biogeochemical measurements were
21 consistently made at 30 m depth. In 2010 collaboration with the UK Met Office led to a
22 redesigned infrastructure, providing simultaneous surface physical and biogeochemical
23 measurements with surface meteorological data.

24 $p(\text{CO}_2)$ data during the two periods of time examined here were collected using
25 different instrumentation. From 2003–2005 it was measured using a SAMI (Sunburst Sensors
26 LLC, USA) sensor, which is based on equilibration of a pH indicator solution, contained in a
27 gas-permeable membrane, with ambient $p(\text{CO}_2)$ and subsequent spectrophotometric
28 determination in the equilibrated solution (DeGrandpre et al., 1995). Twice daily $p(\text{CO}_2)$
29 measurements, from 2010 to 2012, were made using a membrane-based PRO-CO2 sensor
30 (Pro-Oceanus, Canada), which uses an infrared detector and is internally calibrated through

1 an auto-zero calibration function (Jiang et al., 2014). Note that measurement error of early
2 version of PRO-CO₂ sensor during the deployment, induced by the fluctuation of detector
3 cell temperature, was identified and corrected (see Jiang et al., 2014 for further details). A
4 pump was used (Seabird Inc.) to improve water flow across the sensor membrane to
5 accelerate the equilibrium. The surface *in situ* $p(\text{CO}_2)$ time-series ceased between 2006 and
6 2009 and for the early part of 2011.

7 Although measured by different instruments, the two $p(\text{CO}_2)$ data sets were calibrated
8 in a similar way to make them comparable: the sensor outputs were calibrated against $p(\text{CO}_2)$
9 values calculated from dissolved inorganic carbon (DIC) and total alkalinity (TA) from
10 discrete samples taken at the mooring site during deployment/recovery cruises; and
11 plausibility check were made with underway $p(\text{CO}_2)$ measurements around the PAP site. The
12 2003-2005 data were previously published (see Körtzinger et al., 2008 for details) with a
13 precision of 1 μatm and an accuracy estimated as 6-10 μatm . The 2010-2012 data have a
14 similar precision (1 μatm) and accuracy (6 μatm).

15 A Hobi Labs Inc., HS-2 fluorometer (Arizona, USA) was used on the PAP-SO
16 mooring to estimate chlorophyll a until 2005 when an alternative ECO FLNTU (WETlab,
17 USA) fluorometer came into use. The quoted precision for these fluorometers is 0.04%,
18 however as described by Hartman et al., (2010), fluorescence output can only provide an
19 approximation of chlorophyll a. The fluorescence/chlorophyll a calibration ratio changes
20 throughout the year, due to variations in the phytoplankton species composition. On the
21 mooring, chlorophyll a-fluorescence measurements were taken every 2 hours over the 1 year
22 deployments and biofouling was controlled using motorised copper shutters on each of the
23 fluorometers.

24 Nitrate concentration measurements were initially made using wet chemical NAS
25 Nitrate Analysers (EnviroTech LLC, USA), precision 0.2 $\mu\text{mol l}^{-1}$, as described in Hydes et
26 al. (2000), with twice daily sampling frequency and internal calibration as described by
27 Hartman et al. (2010). From 2010 additional higher frequency inorganic nitrate
28 measurements were made using UV detection methods (ISUS, Satlantic), with a precision of
29 1 $\mu\text{mol l}^{-1}$.

30 For each instrument the manufacturer's calibration was checked at the start of each
31 deployment and a correction for instrument drift was made using a second calibration check
32 on recovery of the instruments. Biogeochemical data from the PAP-SO are available from

1 www.eurosites.info/pap and the British Oceanographic Data Centre (BODC). Data presented
2 here cover the period when $p(\text{CO}_2)$ measurements are available, July 2003 to the end of June
3 2005 (with deployments in July 2003, November 2003, June 2004) and the period from May
4 2010 to June 2012 (with sensor deployment in May 2010, September 2010, July 2011, May
5 2012). All of the measurements are within the mixed layer although the depth of
6 measurements is closer to the 30 m nominal depth after mooring redesign to incorporate a
7 surface float in 2007.

8

9 **2.3 Other observational data sources**

10 Temperature and salinity data were taken from Argo floats
11 (<http://www.coriolis.eu.org>), extracting 30 (± 5) m depth data. To obtain a continuous
12 seasonal description, a large region around the PAP site was selected (45° N to 52° N and
13 26.08° W to 8.92° W , excluding the shelf area). The Argo data have a potentially lower
14 accuracy (0.005° C for temperature and 0.1 for salinity) than the *in situ* microcat data (0.002
15 for salinity and 0.002° C for temperature). A comparison of Argo temperature with *in situ* 30
16 m microcat data ($n=112$, comparison not shown) suggests errors of up to 2 % for salinity and
17 1 % for temperature in the Argo data compared with the *in situ* data (when available).
18 However the Argo data were chosen over the *in situ* data as they have a larger temporal
19 coverage and are internally consistent.

20 The $p(\text{CO}_2)$ time-series was compared with surface data from a ship of opportunity
21 (SOO) running from Portsmouth, UK to the Caribbean (Schuster et al., 2007). Onboard the
22 SOO continuous $p(\text{CO}_2)$ measurements are made using a calibrated system with a
23 showerhead equilibrator (Schuster et al., 2007). Discrete nutrient samples were collected at 4
24 hour intervals along the route and were analysed ashore (Hartman et al., 2008). This provides
25 an approximately monthly nutrient sample and $p(\text{CO}_2)$ data points close to the PAP-SO on
26 the return route of the ship. The nominal depth of these samples is 5 m, which is shallower
27 than the 30 m samples from the PAP-SO. We selected SOO data between 52° N and 45° N
28 and 8.92° W and 26.08° W , and then took the average $p(\text{CO}_2)$ values that were within that
29 area on the same day as the sample from the PAP-SO site.

30 Through collaboration with the UK Met Office *in situ* wind speed data are available
31 since 2010. However for consistency in calculations of CO_2 flux between the two time

1 periods (2003–2005 and 2010–2012) considered here we took wind speed data from weekly
2 satellite data: Fleet Numerical Meteorology and Oceanography Center (FNMOC) 1° by 1°.
3 We calculated a weekly mean from the 6 hourly, 10 m height data; available from
4 <http://las.pfeg.noaa.gov/>.

5 The air-sea CO₂ flux (in mmol m⁻² d⁻¹) was calculated from the air-sea $p(\text{CO}_2)$
6 difference, temperature and salinity (30 m) and wind speed at 10 m height, using the
7 following equation:

$$8 \quad F_{\text{CO}_2} = k \cdot K_0 (p\text{CO}_{2\text{sea}} - p\text{CO}_{2\text{air}}) \quad (1)$$

9 Where k is the transfer coefficient based on the wind speed-dependent formulation of
10 Nightingale et al. (2000), scaled to the temperature-dependent Schmidt number according to
11 Wanninkhof (1992), K_0 is the CO₂ solubility at the *in situ* temperature and salinity after
12 Weiss (1974). While $p(\text{CO}_2)_{\text{sea}}$ and $p(\text{CO}_2)_{\text{air}}$ are the CO₂ partial pressures of seawater and
13 air, respectively. As $p(\text{CO}_2)$ was reported throughout this manuscript, we used $p(\text{CO}_2)$ for the
14 air-sea flux calculation. Using $f(\text{CO}_2)$ for calculation would generate the same results of flux
15 estimates. The atmospheric $p(\text{CO}_2)$ is calculated from monthly averaged $x(\text{CO}_2)$ measured at
16 Mace Head (53.33° N, 9.90° W) assuming 100 % water vapour saturation under 1 atm air
17 pressure. Please note that 1 atm = 1.01325 bar.

18 The TA was calculated from Argo temperature and salinity (30 m), following the
19 relationship for the North Atlantic developed by Lee et al. (2006) with an uncertainty of ± 6.4
20 $\mu\text{mol kg}^{-1}$ (Lee et al., 2006). The DIC concentration was then calculated from TA and $p(\text{CO}_2)$
21 using the “seacarb” package (Lavigne and Gattuso, 2011), with Argo temperature and salinity
22 (30 m) and nutrient concentrations set to zero. The chosen constants were Lueker et al.
23 (2000) for K_1 and K_2 , Perez and Fraga (1987) for K_f and the Dickson (1990) constant for K_s ,
24 as recommended by Dickson et al. (2007). Using TA and $p(\text{CO}_2)$ to calculate DIC introduces
25 an error in the order of 6 $\mu\text{mol kg}^{-1}$.

26 The monthly MLD was calculated from density profiles using global gridded fields of
27 temperature and salinity collected by Argo floats, XBTs, CTDs and moorings. These data are
28 collected and made freely available by the Coriolis project and programmes that contribute to
29 it (<http://www.coriolis.eu.org>). We used the near real time mode data as these datasets have
30 been quality control checked. Before deciding on a MLD definition an inter-comparison of
31 many definitions commonly used in the literature was done such as density differences,

1 temperature differences and density gradients (Kara et al. 2000; Thomson and Fine 2003;
2 Montegut et al. 2004). A subset of the global density profiles calculated from the gridded
3 temperature and salinity fields was used to compare the different methods. The depth of the
4 mixed layer was estimated through visual inspection of over 3000 profiles (following a
5 similar approach used by Fiedler (2010)). The Holte and Talley (2009) density difference
6 algorithm gave the closest match with the visually estimated MLD (RMSD 29.38 m). The
7 depth of the mixed layer was defined by a density difference of 0.03 kg m^{-3} from the density
8 at a reference depth (in this case 10 m to avoid diurnal changes in temperature and salinity at
9 the surface). This Holte and Talley (2009) density difference algorithm incorporates linear
10 interpolation to estimate the depth at which the density difference is crossed.

11 The North Atlantic Oscillation (NAO) index (after Hurrell, 1995) was obtained from
12 the University of East Anglia web site <http://www.cru.uea.ac.uk/cru/data/nao/>.

13

14 **3 Results**

15 Figures 2a–c show the *in situ* observations from the PAP-SO at 30 m depth, including
16 $p(\text{CO}_2)$, chlorophyll a-fluorescence and nitrate concentration. Figure 2a shows the range of
17 $p(\text{CO}_2)$ from 2003 to 2005, which was also shown in Körtzinger et al. (2008). The range was
18 $74 \mu\text{atm}$ (300 to $374 \mu\text{atm}$) and the mean was $339 \mu\text{atm}$. In comparison, $p(\text{CO}_2)$ between
19 2010 and 2012 had a $57 \mu\text{atm}$ range (327 to $384 \mu\text{atm}$) with a higher mean value of 353
20 μatm . The $p(\text{CO}_2)$ data for the 2010–2012 period are confirmed by SOO data from the
21 Portsmouth to Caribbean route in Fig. 2a (see Fig. 1 for positions of the SOO samples).
22 Körtzinger et al. (2008) also reported a good comparison with a SOO route from Kiel, to the
23 north of the Portsmouth to Caribbean route, for the 2003–2005 data. The SOO data fill in the
24 gap in the time series when PAP-SO $p(\text{CO}_2)$ data were not available due to failure of the
25 instrument logger. The higher $p(\text{CO}_2)$ values in the 2010 to 2012 period are confirmed by the
26 SOO data.

27 *In situ* chlorophyll data in Fig. 2b shows the characteristic chlorophyll a-fluorescence
28 increase for this area during the spring bloom. There is large inter-annual variability in both
29 the timing and magnitude of the spring bloom for the two time periods shown. For example
30 the spring bloom in 2004 started in late May compared with an earlier bloom in 2011 (that

1 started in April). The spring bloom in 2011 was also larger compared with the other years
2 shown.

3 Nitrate concentration data in Fig. 2c shows the characteristic seasonality, with
4 increased winter nitrate concentrations and depletion following the spring bloom (seen in Fig.
5 2b). The seasonality in the nitrate concentration is similar for the two periods shown (2003–
6 2005 and 2010–2012). SOO nitrate concentration data show a good agreement with the PAP-
7 SO data throughout 2010–2012 and fill in the gaps in early 2011 when nutrient measurements
8 at the PAP-SO are not available.

9 Overall, the *in situ* data show a characteristic increase in inorganic nitrate
10 concentrations, and $p(\text{CO}_2)$, through the winter as fluorescence decreases. However, winter
11 nitrate concentrations are significantly lower in the 2004/2005 winter compared with other
12 years as has been discussed in Hartman et al., (2010).

13 Fig. 3a shows the Argo temperature data extracted at 30 m depth, which shows an
14 opposite trend to the $p(\text{CO}_2)$ and nitrate concentration from *in situ* data. The temperature
15 variations in these years are very similar showing a summer-winter difference of 6 °C. The
16 MLD range varies little over the winters considered here (Fig. 3b) and the maximum MLD
17 does not exceed 260 m. However the timing of the maximum winter mixed layer depth varies
18 from year to year. For example the maximum MLD for the 2010/2011 winter reached 215 m
19 in February 2011 compared with earlier and deeper mixing (to 257 m) in the following
20 2011/2012 winter (December 2011).

21 The seasonality of the *in situ* data can be put in context when looking at the MLD in
22 Fig. 3b. The increase in winter nitrate concentration and $p(\text{CO}_2)$ due to convective mixing at
23 the site is shown. The calculated DIC concentrations (Fig. 3c) show a closer relationship to
24 the MLD seasonality than nitrate concentration data. Seasonal variation in the concentration
25 of both DIC and nitrate is similar apart from the 2004/2005 winter; when low DIC
26 concentrations were not seen at the same time as the low nitrate concentrations.

27 The interrelation between DIC and nitrate concentrations for the 2010-2012 time
28 period can be considered by comparing the C: N ratios to the Redfield ratio (Redfield, 1958),
29 which is illustrated in Fig. 4. The 2003-2005 time period has already been considered in
30 Körtzinger et al. (2008) so is not reproduced here. The changes in calculated DIC
31 concentrations (corrected for the changes due to air-sea CO_2 exchange) at the PAP-SO, in

1 relation to changes in the *in situ* nitrate concentrations for 2010-2012, are represented for the
2 different seasons. The C: N ratio differed from the Redfield ratio of 6.6 with especially high
3 values in spring (14.3).

4 Figure 5a shows weekly satellite wind speed data used to calculate the CO₂ flux. The
5 wind speeds were similar in the two periods. There is an earlier period of days with high wind
6 speeds towards the end of 2011 that can be compared with the CO₂ data presented. The
7 annual average wind speed was 8.2 m s⁻¹ for both time periods. The maximum was 14 m s⁻¹,
8 although *in situ* winds of up to 20 m s⁻¹ were seen from the Met Office data
9 (eurosites.info/pap), this is not seen in the weekly averaged satellite wind speed data
10 presented.

11 Figure 5b shows the sea-to-air CO₂ flux (where a positive flux is defined as from sea
12 to the atmosphere). This was calculated from *in situ* p(CO₂) data and satellite wind speed data
13 (Fig. 5b). The week by week variation in CO₂ flux is shown and an overall average for the
14 two periods of time has been calculated as -5.7 ± 2.8 mmol m⁻² d⁻¹ for the 2003–2005 period
15 and -5.0 ± 2.2 mmol m⁻² d⁻¹ for the 2010–2012 period.

16 There is little variation in CO₂ flux and MLD between the years shown but for
17 completeness the NAO index is shown in Fig. 5c. The 2003/2004 winter NAO was near zero
18 and the 2004/2005 winter NAO was also low, between -2 to +1. In contrast there is a large
19 range in the winter NAO in the 2010/2011 winter when the NAO changed from -4 to +3.
20 Also in the winter of 2011/2012 there was a relatively high NAO of +3. Overall the range in
21 the NAO values was larger for the 2010 to 2012 time period shown.

22

23 **4 Discussion**

24 **4.1 PAP-SO seasonal variation**

25 The 2003–2005 and 2010–2013 datasets show very similar seasonal patterns between
26 the years. Concentrations of nitrate and DIC exhibit a seasonality, which varied inversely
27 with temperature. The seasonal variation in nitrate and DIC concentrations is controlled by
28 the convective mixing (resulting in the winter maximum) and biological uptake during the
29 spring bloom period (resulting in the summer minimum), which is similar to elsewhere in
30 North Atlantic (Jiang et al. 2013).

1 The $p(\text{CO}_2)$ distribution pattern at the PAP-SO site is characterized by a single annual
2 peak (high in winter and low in summer), which is similar to that of nutrient and DIC
3 concentrations, but in antiphase to the temperature signal. Jiang et al. (2013) compared
4 seasonal carbon variability between different sites in the North Atlantic and suggested a
5 latitudinal change in the $p(\text{CO}_2)$ seasonality from the temperature-dominated oligotrophic
6 subtropical gyre to the subpolar region where $p(\text{CO}_2)$ is dominated by changing
7 concentrations of DIC. Our $p(\text{CO}_2)$ observations at the PAP-SO site show the subpolar-like
8 seasonal pattern, which is similar to that of the Ocean Weather Station M (Skjelvan et al.,
9 2008). The surface $p(\text{CO}_2)$ is mainly governed by the varying DIC concentration while the
10 seasonal cooling and warming have a contrasting effect.

11 The time integrated uptake of DIC and nitrate during the spring bloom is reflected by
12 the slope of the linear regression between them (Fig. 4). The ratio of DIC and nitrate
13 concentrations from 2010-2012 shows higher values than the Redfield C : N ratio of 6.6. For
14 example the spring-time ratio of 14.3 (± 5) was considerably higher than the Redfield ratio, in
15 agreement with similar “carbon overconsumption” ratios seen for the North Atlantic (e.g.
16 14.2, Sambrotto et al., 1993). It is also in agreement with the single C : N ratio reported
17 previously at the PAP-SO of 11.0 (Körtzinger et al., 2008). We have demonstrated seasonal
18 variation in the C : N ratio at the PAP-SO, with an autumn C : N value that is closer to the
19 Redfield ratio and large deviations from the Redfield ratio in winter.

20

21 **4.2 Air-sea CO₂ flux**

22 Wind speeds have an indirect impact on the biogeochemistry, in particular the $p(\text{CO}_2)$.
23 In the North Atlantic long-term wind speed is increasing and the intensity of storms is
24 predicted to increase (Knutson et al., 2012). Wind speeds are similar for the two time periods
25 considered here. However there is some suggestion of an earlier increase in winds at the start
26 of the 2011/2012 winter (Fig. 5a) coinciding with an earlier increase in mixing (Fig. 3b).
27 Although the CO₂ flux is not linked linearly to the wind speed there is a corresponding
28 decrease in CO₂ flux into the ocean at this time.

29 It is well known that the northeast Atlantic is a strong CO₂ sink with large variability.
30 The observations at the PAP-SO provide high frequency data to follow the variability in CO₂
31 exchange. The largest CO₂ flux shown here was in September 2004, as a combined result of

1 low seawater $p(\text{CO}_2)$ (Fig. 2a) and high wind speed (Fig. 5b). Larger CO_2 flux into the ocean
2 may have occurred in 2011 considering the large, early spring bloom seen in that year but we
3 do not have $p(\text{CO}_2)$ data to calculate the flux at that time. The average CO_2 flux is lower in
4 the 2010–2012 period, although again this may be biased by the missing data in early 2011.
5 However, increases in productivity do not necessarily result in enhanced oceanic CO_2 uptake
6 as the gas exchange is also affected by other factors such as temperature and wind speed
7 (Dumousseaud et al., 2010; Jiang et al., 2013). The average is similar for the years presented
8 with values of $-5.7 \text{ mmol m}^{-2} \text{ d}^{-1}$ in 2003–2005 and $-5.0 \text{ mmol m}^{-2} \text{ d}^{-1}$ from 2010–2012.

9

10 **4.3 PAP-SO inter-annual variations**

11 It is suggested that NAO plays an important role in modulating the inter-annual
12 variability in northeast Atlantic region by affecting the intensity of winter convection
13 (Bennington et al., 2009; Jiang et al. 2013). The Gibraltar minus Iceland version of the NAO
14 index is really most applicable to the winter half of the year. During positive NAO periods,
15 the PAP-SO region experiences subpolar-like conditions, with strong wind stress and deep
16 mixed layers (Henson et al., 2012). However the MLD did not vary significantly at the PAP-
17 SO between the 2003–2005 and 2010–2012 time periods shown here (with a range of only
18 215 to 257 m for deepest winter MLD between the years, when in previous years such as
19 2009/2010 deep winter mixing of 390 m has been seen with an NAO reaching -3 , not
20 shown). So NAO is unlikely to have a large role as the PAP-SO winter sea surface
21 temperature and MLD were similar in the time periods from 2003–2005 and 2010–2013.
22 Data from a winter with deeper mixing would need to be put into the comparison to resolve
23 this.

24 However, there was a twofold decrease in nitrate concentrations in the 2004/05 win-
25 ter despite sea surface temperature and MLD values being close to other years. The low
26 values were confirmed by SOO data in Hartman et al. (2010). As discussed in Hartman et al.
27 (2010) the lower winter nitrate concentration seen in 2004/2005 did not correlate with a
28 decrease in the MLD and this showed the influence of horizontal mixing at the PAP-SO. It
29 was suggested that lateral advection to the site at that time introduced a subtropical water
30 mass with a lower nitrate concentration. Earlier time-series studies largely ignored circulation
31 at the PAP-SO site, assuming convective mixing is a dominant process influencing mixed
32 layer temperature and nitrate concentrations in the region (Williams et al., 2000; Körtzinger

1 et al. 2008). However, fixed-point time-series observations are influenced by spatial
2 variability passing the point of observation (McGillicuddy et al., 1998; Painter et al., 2010). It
3 is clear from Hartman et al. (2010) that lateral advection may significantly influence the
4 surface temperature and nitrate concentrations in the region of the PAP-SO site.

5 The observed seawater $p(\text{CO}_2)$ increased from $339 \pm 17 \mu\text{atm}$ in 2003-2005 to $353 \pm$
6 $15 \mu\text{atm}$ in 2010-2012, which largely agrees with the increasing rate of surface seawater
7 $p\text{CO}_2$ observed in the North Atlantic basin ($1.84 \pm 0.4 \mu\text{atm a}^{-1}$, Takahashi et al. 2009).
8 Despite similar maximum winter MLD in 2003–2005 and 2010–2013, the timing and
9 intensity of the spring bloom is also quite different. The cause of these differences requires
10 further investigation.

11

12 **5 Conclusions and further work**

13 We have presented recent year round surface time-series biogeochemical data at the
14 PAP-SO and compared it with previous observations. The surface $p(\text{CO}_2)$, and concentrations
15 of DIC and nitrate, all show a clear seasonal cycle, which is mainly controlled by winter
16 convective mixing and biological activity in the spring bloom. However the suggestion that
17 inter-annual variability is dominated by convection (Bennington et al., 2009) is not clear as
18 the MLD did not vary significantly between the winter periods shown. An especially low
19 winter nitrate concentration in 2005 was observed thought to be due to surface advection and
20 this highlights the need to consider advection when dealing with time series data. Despite the
21 similar winter physical conditions (temperature and MLD), the differences in timing and
22 intensity of the spring blooms requires further investigation. At the PAP-SO, increasing mean
23 seawater $p(\text{CO}_2)$ from 2003 to 2011 ($339 \pm 17 \mu\text{atm}$ to $353 \pm 15 \mu\text{atm}$) was observed. The
24 mean air-sea CO_2 flux did not show a significant change ($-5.7 \pm 2.8 \text{ mmol m}^{-2} \text{ d}^{-1}$ to $-5.0 \pm$
25 $2.2 \text{ mmol m}^{-2} \text{ d}^{-1}$).

26 In 2010, collaboration between the UK's Natural Environment Research Council
27 (NERC) and Meteorological Office led to the first simultaneous monitoring of *in situ*
28 meteorological and ocean variables at the PAP-SO (Hartman et al., 2012). From 2013
29 additional measurements of $p(\text{CO}_2)$ will be made at the site, at the shallower depth of 1 m,
30 and should further improve the SOO comparison. The site could be used to investigate the
31 effect of different parameterizations (Prytherch et al., 2010) and wind products on

1 calculations of CO₂ flux, in particular during the high wind conditions seen. Using the
2 contemporaneous atmospheric and ocean datasets we will be able to investigate the effect of
3 the storms on CO₂ flux and resolve daily variability.

4

5 **Acknowledgements**

6 We would like to acknowledge the various ship crew, engineers and scientists involved in
7 preparation, deployment and recovery of the PAP-SO moorings. We would especially
8 like to thank J. Campbell, M. Hartman and M. Pagnani for the PAP time series and H. Cole
9 who calculated MLD from the Argo float data. The research leading to these results was
10 supported through the EU FP7 project CARBOCHANGE “Changes in carbon uptake and
11 emissions by oceans in a changing climate”, which received funding from the European
12 Commission’s Seventh Framework Programme under grant agreement no. 264879. Funding
13 that supports the running of the SOO network used in this project also includes EU grant
14 212196 (CO- COS), and UK NERC grant NE/H017046/1 (UKOARP); Funding for part of
15 this study was provided by NERC CASE studentship grant reference number NE/J500069/1
16 in collaboration with SAHFOS. Argo data were made freely available by the Coriolis project
17 and programmes that contribute to it <http://www.coriolis.eu.org>. FNMOC wind speed data
18 were available from <http://las.pfeg.noaa.gov>. Mooring data and support for this research was
19 provided by the European research projects ANIMATE (Atlantic Network of
20 Interdisciplinary Moorings and Time- Series for Europe), MERSEA (Marine Environment
21 and Security for the European Sea), EUR- OCEANS (European Network of Excellence for
22 Ocean Ecosystems Analysis) and EuroSITES grant agreement EU 202955. The work was
23 also supported through the Natural Environment Research Council (NERC), UK, project
24 Oceans 2025 and National Capability. The PAP-SO also contributes to the EU funded FixO3
25 project EU 312463 and the NERC Greenhouse Gas TAP NE/k00249x/1. D. Turk was
26 supported by the Canada Excellence Research Chair (CERC) in Oceans Science and
27 Technology. LDEO contribution number 7768.

28

29 **References**

30

- 1 Behrenfeld, M. J., O'Malley, R. T., Siegel, D. A., McClain, C. R., Sarmiento, J. L., Feldman,
2 G. C., and Milligan, A. J.: Climate-driven trends in contemporary ocean productivity, *Nature*,
3 444, 752–755, 2006.
- 4 Bennington, V., McKinley, G. A., Dutkiewicz, S., and Ullman, D.: What does chlorophyll
5 variability tell us about export and air-sea CO₂ flux variability in the North Atlantic?, *Global*
6 *Biogeochem. Cy.*, 23, GB3002, doi:10.1029/2008GB003241., 2009.
- 7 DeGrandpre, M. D., Hammar, T. R., Smith, S. P., and Sayles, F. L.: In situ measurements of
8 seawater pCO₂, *Limnol. Oceanogr.*, 40, 969–975, 1995.
- 9 Dickson, A. G.: Standard potential of the (AgCl(s) + 1/2H₂(g)=Ag(s) + HCl(aq)) cell and
10 the dissociation constant of bisulfate ion in synthetic sea water from 273.15 to 318.15 K, *J.*
11 *Chem. Thermodyn.*, 22, 113–127, doi:10.1016/0021-9614(90)90074-Z, 1990.
- 12 Dickson, A. G., Sabine, C. L., and Christian, J. R.: Guide to Best Practices for Ocean CO₂
13 Measurements, PICES Special Publication 3, Sidney, British Columbia. 191 pp., 2007.
- 14 Fiedler, P.C.: Comparison of objective descriptions of the thermocline. *Limnology and*
15 *Oceanography-Methods*, 8, 313-325, 2010.
- 16 Field, C. B., Behrenfeld, M. J., and Randerson, J. T.: Primary production of the biosphere:
17 integrating terrestrial and oceanic components, *Science*, 281, 237–240, 1998.
- 18 González-Dávila, M., Santana-Casiano, J. M., Rueda, M. J., Llinas, O., and Gonzalez-
19 Davila, E. F.: Seasonal and interannual variability of sea-surface carbon dioxide species at the
20 European Station for Time Series in the Ocean at the Canary Islands (ESTOC) between 1996
21 and 2000., *Global Biogeochem. Cy.*, 17, 1076, doi:10.1029/2002gb001993, 2003.
- 22 Hartman, S. E., Larkin, K. E., Lampitt, R. S., Lankhorst, M., and Hydes, D. J.: Seasonal and
23 inter-annual biogeochemical variations in the Porcupine Abyssal Plain 2003–2005 associated
24 with winter mixing and surface circulation, *Deep-Sea Res. II*, 57, 1303–1312, 2010.
- 25 Hartman, S. E., Lampitt, R. S., Larkin, K. E., Pagnani, M., Campbell, J., Gkritzalis, A., and
26 Jiang, Z. P.: The Porcupine Abyssal Plain fixed-point sustained observatory (PAP-SO):
27 variations and trends from the Northeast Atlantic fixed-point time-series, *ICES J. Mar. Sci.*,
28 57, 776–783, 2012.

- 1 Henson, S., Lampitt, R., and Johns, D.: Variability in phytoplankton community structure in
2 response to the North Atlantic Oscillation and implications for organic carbon flux, *Limnol.*
3 *Oceanogr.*, 57, 1591, 2012.
- 4 Holte, J. and Talley, L.: A New Algorithm for Finding Mixed Layer Depths with
5 Applications to Argo Data and Subantarctic Mode Water Formation, *J. Atmos. Ocean. Tech.*,
6 26, 1920–1939, 2009.
- 7 Hurrell, J. W.: Decadal trends in the North Atlantic oscillation: regional temperatures and
8 precipitation, *Science*, 269, 676–679, 1995.
- 9 Hydes, D. J., Wright, P. N., and Rawlinson, M. B.: Use of a wet chemical analyser for the *in*
10 *situ* monitoring of nitrate, *Chemical sensors in Oceanography*, in: *Chemical Sensors in*
11 *Oceanography*, edited by: Varney, M., Gordon and Breach, Amsterdam, 95–105, 2000.
- 12 Jiang, Z-P, Hydes, D.J, Tyrrell, T., Hartman, S. E., Hartman, M. C., Dumousseaud, C., Padin,
13 X. A., Skjelvan, I., and González-Pola, C.: Key controls on the seasonal and inter- annual
14 variations of the carbonate system and air-sea CO₂ flux in the Northeast Atlantic (Bay of
15 Biscay), *J. Geophys. Res.-Oceans*, 118, 785–800, 2013.
- 16 Jiang, Z-P, Hydes, D.J, Tyrrell, T., Hartman, S. E., Hartman, M. C., Campbell, J. M.,
17 Johnson, B. D., Schofield, B., Turk, D., Wallace, D, Burt, W., Thomas, H., Cosca, C., and
18 Feely, R.: Application and assessment of a membrane-based pCO₂ sensor under field and
19 laboratory conditions, *Limnol. Oceanogr.-Meth.*, 12, 264–280, 2014.
- 20 Kara, A.B., Rochford P.A. and Hurlburt H.E.: An optimal definition for ocean mixed layer
21 depth. *Journal of Geophysical Research-Oceans*, 105(C7), 16803-16821, 2000.
- 22 Knutson, T.R., McBride, J.L., Chan, J., Emanuel, K., Holland, G., Landsea, C., Held, I.,
23 Kossin, J.P., Srivastava, A.K, and Sugi, M.: Tropical cyclones and climate change. *Nature*
24 *Geoscience*, 3, 157-163, 2010.
- 25 Körtzinger, A., Send, U., Lampitt, R.S., Hartman, S., Wallace, D. W. R., Karstensen, J.,
26 Villagarcia, M. G., Llinás, O., and DeGrandpre, M. D.: The seasonal pCO₂ cycle at 49°
27 N/16.5° W in the northeastern Atlantic Ocean and what it tells us about biological
28 productivity, *J. Geophys. Res.*, 113, C04020, doi:10.1029/2007jc004347, 2008.

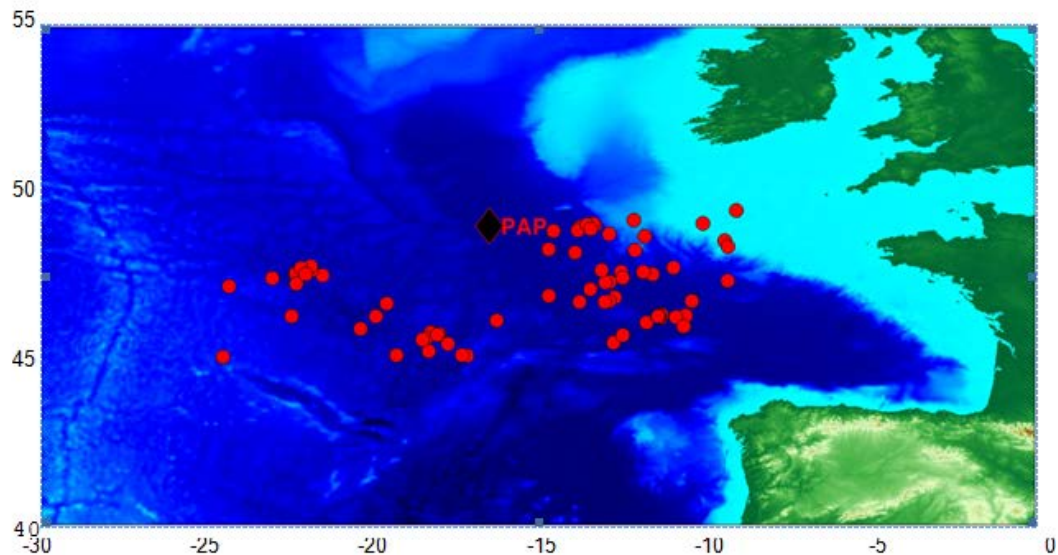
- 1 Lampitt, R. S., Bett, B. J., Kiriakoulis, K., Popova, E., Ragueneau, O., Vangriesheim, A., and
2 Wolff, G. A.: Material supply to the abyssal seafloor in the Northeast Atlantic, *Prog.*
3 *Oceanogr.*, 50, 27–63, 2001.
- 4 Lavigne, H. and Gattuso, J.-P.: Seacarb: seawater carbonate chemistry with R. R package
5 version 2.4., [http://CRAN.R-project.org/package=seacarb.](http://CRAN.R-project.org/package=seacarb), edited., 2011.
- 6 Lee, K., Tong, L. T., Millero, F. J., Sabine, C. L., Dickson, A. G., Goyet, C., Park, G. H.,
7 Wanninkhof, R., Feely, R. A., and Key, R. M.: Global relationships of total alkalinity with
8 salinity and temperature in surface waters of the world's oceans, *Geophys. Res. Lett.*, 33,
9 L19605,doi:10.1029/2006gl027207, 2006.
- 10 Longhurst, A.: Ecological geography of the sea, *Ecological Geography of the Sea Series*, 2nd
11 ed., 560 pp., Academic Press, San Diego, 2006.
- 12 Lueker, T. J., Dickson, A. G. and Keeling, C. D.: Ocean pCO₂ calculated from dissolved in-
13 organic carbon, alkalinity, and equations for K-1 and K-2: validation based on laboratory
14 measurements of CO₂ in gas and seawater at equilibrium, *Mar. Chem.*, 70, 105–119, 2000.
- 15 McGillicuddy, D. J., Robinson, A. R., Siegel, D. A., Jannasch, H. W., Johnson, R., Dickey,
16 T. D., McNeil, J., Michaels, A. F., and Knap, A. H.: Influence of mesoscale eddies on new
17 production in the Sargasso Sea, *Nature*, 394, 263–266, 1998.
- 18 McKinley, G. A., Fay A. R., Takahashi T., and Metzl, N.: Convergence of atmospheric and
19 North Atlantic carbon dioxide trends on multidecadal timescales. *Nature geoscience*, 4 (9),
20 606-610, 2011.
- 21 Montegut, C.D., Madec, G., Fischer, A.S., Lazar, A. and Iudicone D.: Mixed layer depth over
22 the global ocean: An examination of profile data and a profile-based climatology. *Journal of*
23 *Geophysical Research-Oceans*. 109, C18, 12003, 2004.
- 24 Monterey, G. and Levitus, S.: Seasonal variability of mixed layer depth for the World Ocean,
25 NOAA NESDIS Atlas, US Government Printing Office, Washington, DC, 5 pp., 1997.
- 26 Nightingale, P. D., Malin, G., Law, C. S., Watson, A. J., Liss, P. S., Liddicoat, M. I., Boutin,
27 J., and Upstill-Goddard R. C.: In situ evaluation of air-sea gas exchange parameterizations
28 using novel conservative and volatile tracers, *Global Biogeochem. Cy.*, 14, 373–387,
29 doi:10.1029/1999GB900091, 2000.

- 1 Padin, X. A., Castro, C. G., Ríos, A. F., and Pérez, F. F.: Oceanic CO₂ uptake and
2 biogeochemical variability during the formation of the Eastern North Atlantic Central water
3 under two contrasting NAO scenarios, *J. Marine. Syst.*, 84, 96–105, 2011.
- 4 Painter, S. C., Pidcock, R. E., and Allen, J. T.: A mesoscale eddy driving spatial and temporal
5 heterogeneity in the productivity of the euphotic zone of the Northeast Atlantic, *Deep-Sea*
6 *Res. II*, 57, 1281–1292, 2010.
- 7 Perez, F. F., Mourin C., Fraga, F., and Rios, A. F.: Displacement of water masses and
8 remineralization rates off the Iberian Peninsula by nutrient anomalies, *J. Mar. Res.*, 51, 869–
9 892, 1993.
- 10 Prytherch, J., Yelland, M. J., Pascal, R. W., Moat, B. I., Skjelvan, I., and Neill, C. C.: Direct
11 measurements of the CO₂ flux over the ocean: development of a novel method, *Geophysical*
12 *Research Letters*, 37, doi:10.1029/2009GL041482, 2010.
- 13 Redfield, A. C.: The biological control of chemical factors in the environment, *American*
14 *scientist*, 64, 205–221, 1958, 1958.
- 15 Schuster, U. and Watson, A. J.: A variable and decreasing sink for anthropogenic CO₂ in the
16 North Atlantic, *J. Geophys. Res.-Oceans*, 112, C1106, doi:10.1029/2006JC003941, 2007.
- 17 Schuster, U., Watson, A. J., Bates, N. R., Corbiere, A., Gonzalez-Davila, M. Metzl, N.,
18 Pierrot, D., and Santana-Casiano, M.: Trends in North Atlantic sea-surface fCO₂ from 1990
19 to 2006, *Deep-Sea Res. II*, 56, 620–629, doi:10.1016/j.dsr2.2008.12.011, 2009.
- 20 Skjelvan, I., Falck, E., Rey, F., and Kringstad, S. B.: Inorganic carbon time series at
21 OceanWeather Station M in the Norwegian Sea, *Biogeosciences*, 5, 549–560,
22 doi:10.5194/bg-5-549-2008, 2008.
- 23 Takahashi, T., Sutherland, S. C., Wanninkhof, R., Sweeney, C., Feely, R. A., Chipman, D.
24 W., Hales, B., Friederich, G., Chavez, F., Sabine, C., Watson, A., Bakker, D. C. E., Schuster,
25 U., Metzl, N., Yoshikawa-Inoue, H., Ishii, M., Midorikawa, T., Nojiri, Y., Kortzinger, A.,
26 Steinhoff, T., Hoppema, M., Olafsson, J., Arnarson, T. S., Tilbrook, B., Johannessen, T.,
27 Olsen, A., Bellerby, R., Wong, C. S., Delille, B., Bates, N. R. and de Baar H. J. W.
28 Climatological mean and decadal change in surface ocean pCO₂, and net sea-air CO₂ flux
29 over the global oceans, *Deep-Sea Res., Pt II*, 56(8-10), 554-577, doi:
30 10.1016/j.dsr2.2008.12.009, 2009.

- 1 Takahashi, T., Sutherland, S. C., Sweeney, C., Poisson, A., Metzl, N., Tilbrook, B., and
2 Bates, N.: Global sea–air CO₂ flux based on climatological surface ocean pCO₂, and
3 seasonal biological and temperature effects, *Deep-Sea Res. II*, 49, 1601–1622, 2002.
- 4 Thomson, R.E. and Fine, I.V.: Estimating Mixed Layer Depth from Oceanic Profile Data.
5 *Journal of Atmospheric and Oceanic Technology*, 20(2), 319-329, 2003.
- 6 Wanninkhof, R.: Relationship between wind-speed and gas-exchange over the ocean, *J. Geo-*
7 *phys. Res.*, 97, 7373–7382, doi:10.1029/92JC00188, 1992.
- 8 Weiss, R. F.: Carbon dioxide in water and seawater: the solubility of a non-ideal gas,
9 *Mar.Chem.*, 2, 203–215, doi:10.1016/0304-4203(74)90015-2, 1974.
- 10 Williams, R. G., McLaren, A. J., and Follows, M. J.: Estimating the convective supply of
11 nitrate and implied variability in export production over the North Atlantic, *Global*
12 *Biogeochem. Cy.*, 14, 1299–1313, 2000.

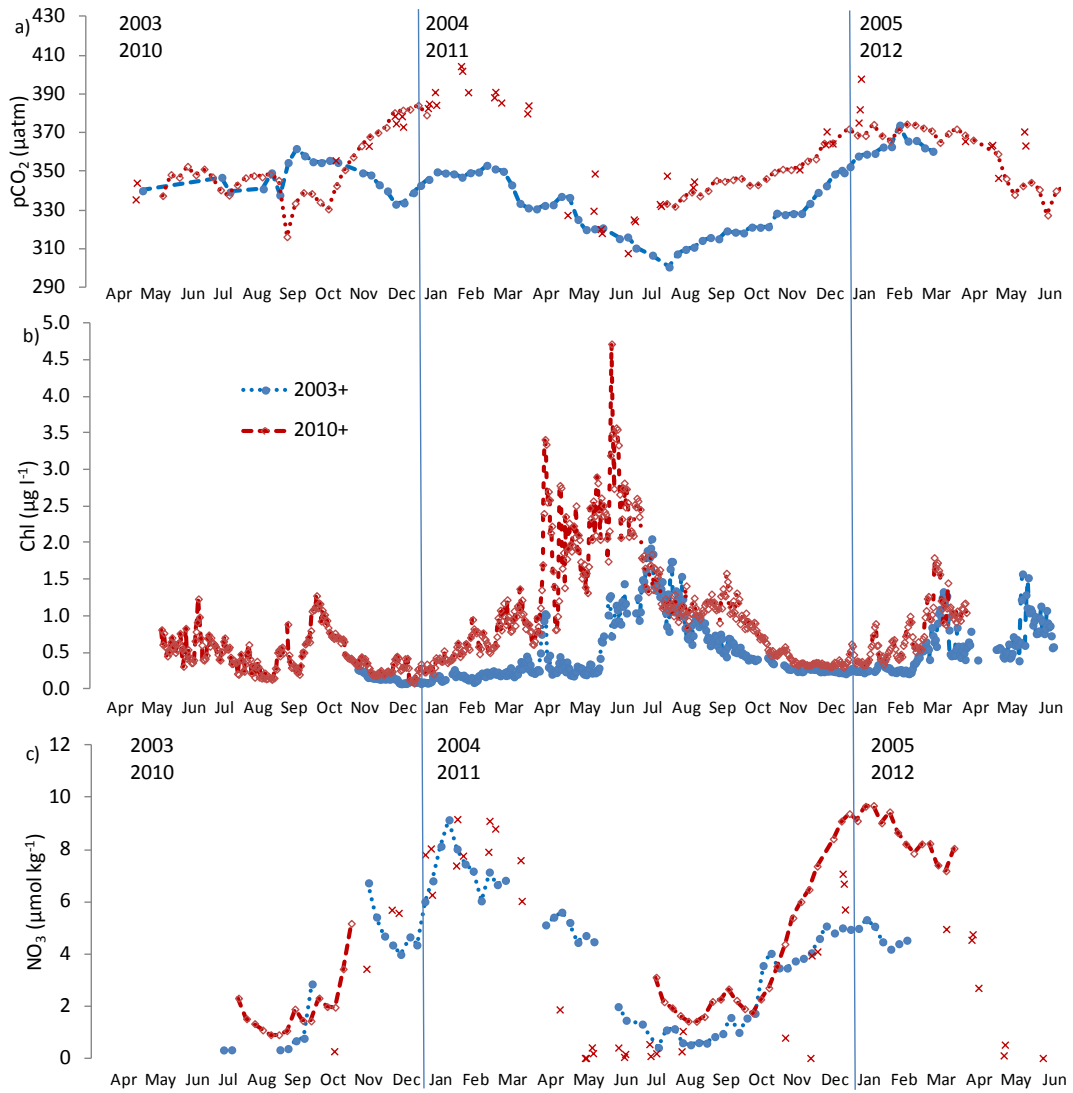
13

14



15

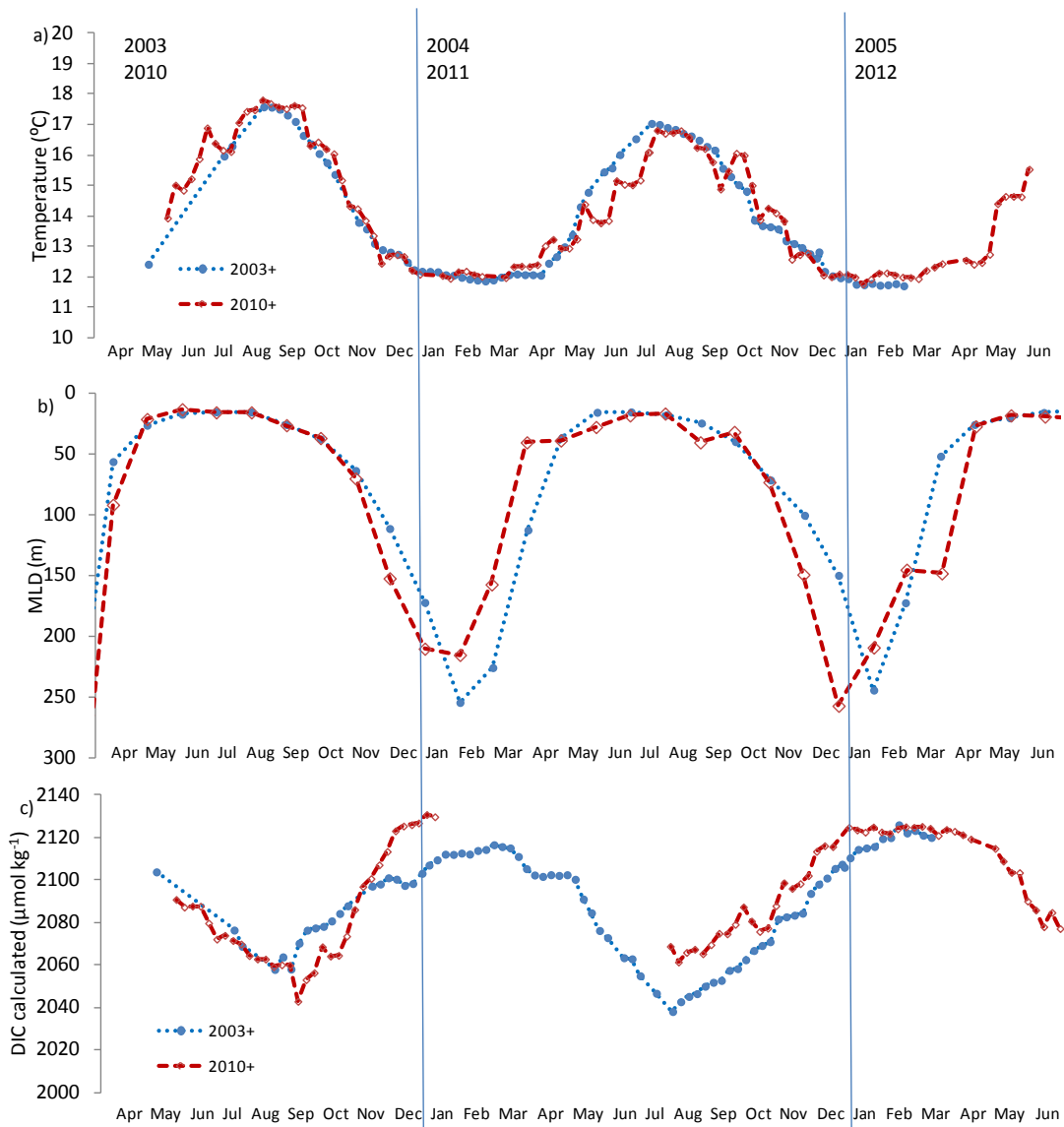
16 Figure 1. Map of the inter-gyre region of the northeast Atlantic showing the
17 bathymetry around the PAP observatory (black diamond) and the ship of opportunity (SOO)
18 sampling positions (red circles) from 2010 to 2012.



1
 2
 3
 4
 5
 6
 7
 8

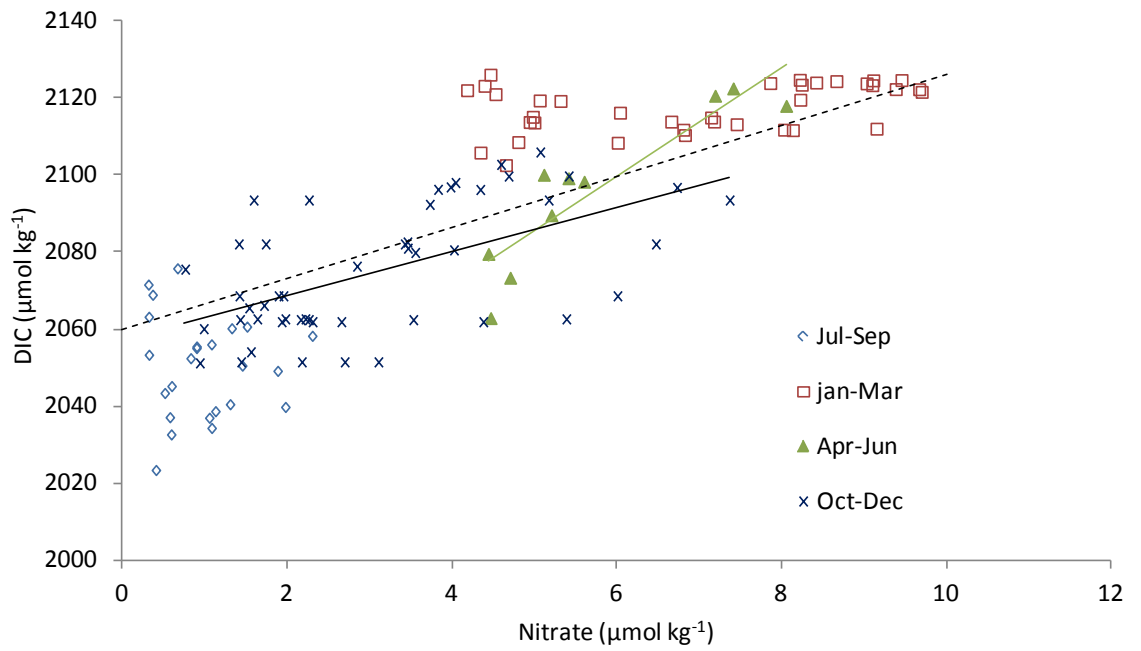
Figure 2. *In situ* 30 m PAP-SO data from 2003–2005 (blue circles), 2010–2012 (red diamonds) and 5 m SOO data from 2010–2012 (red crosses) with vertical lines to represent the start of each year showing: (a) $p(\text{CO}_2)$; (b) chlorophyll a; (c) weekly *in situ* nitrate concentration.

1



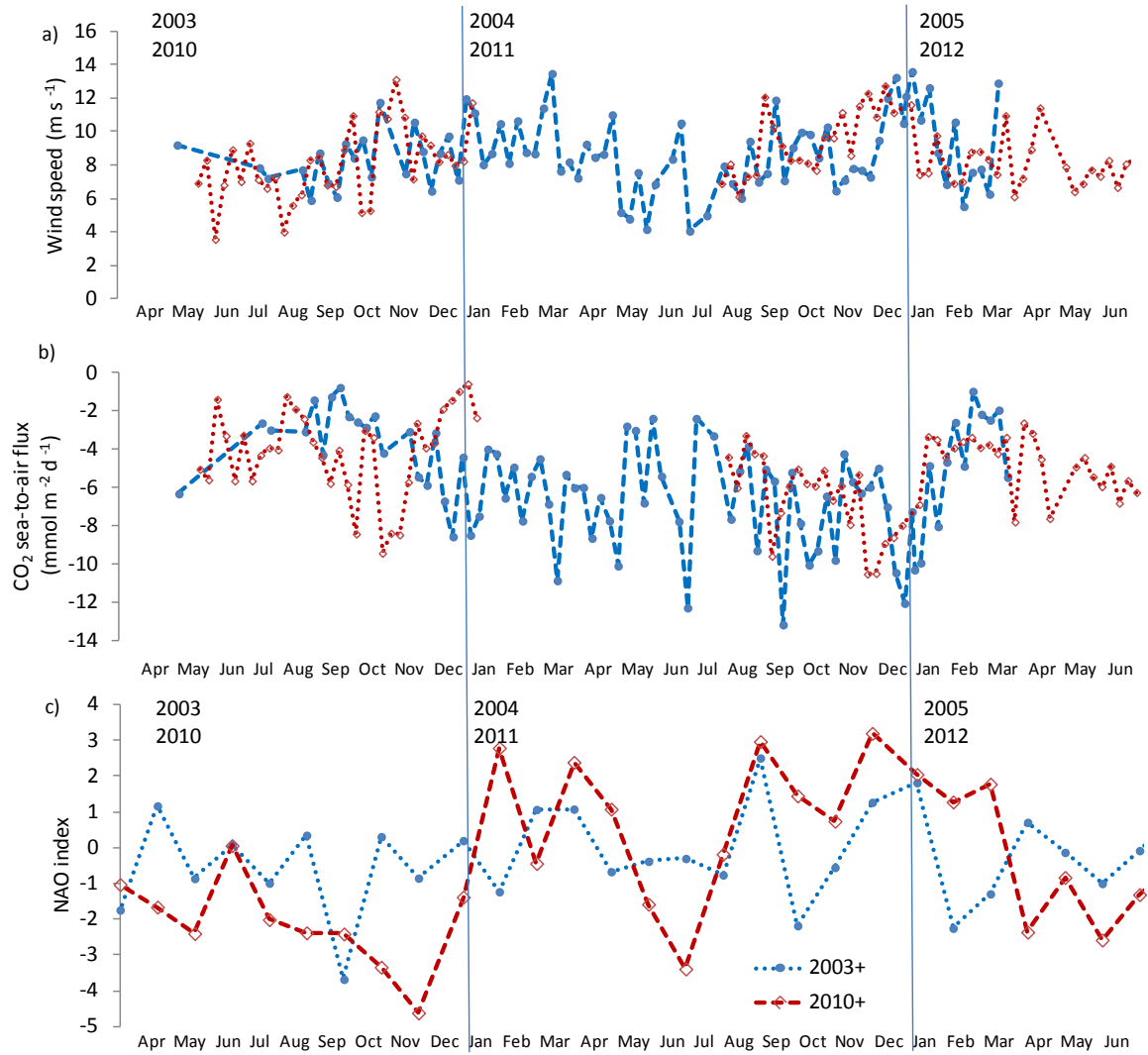
2
3

4 Figure 3. Data from 2003–2005 (blue circles) and 2010–2012 (red diamonds) with
5 vertical lines to represent the start of each year showing: (a) Argo temperature data from 30
6 m depth around the PAP-SO; (b) monthly mixed layer depth (MLD) data; (c) calculations of
7 weekly dissolved inorganic carbon (DIC) concentrations.



1
2

3 Figure 4. The relationship between concentrations of gas exchange-corrected DIC and
 4 nitrate (2010-2012) at the PAP-SO showing 4 different seasons: Winter (January–March, red
 5 squares); Spring (April-June, green triangles); Summer (July-September, blue diamonds);
 6 Autumn (October to December, dark blue crosses). The green line shows the ratio in spring
 7 (14.3) and the blue line is the ratio in autumn (6.4), with the Redfield ratio of 6.6 shown for
 8 reference as a dashed line.



1
2

3 Figure 5: PAP-SO data from 2003-2005 (blue circles) and 2010-2012 (red diamonds) for (a)
 4 weekly satellite wind data; b) calculations of weekly sea-to-air CO₂ flux (negative: into the
 5 ocean); c) the monthly NAO index.

6